Inexpensive Interferometric Wavemeter
for Visible/NIR Lasers

and

Rovibronic Spectrum of the A-X 2-1 Band of N_2^+
Utilizing Cavity Ringdown Spectroscopy
by

Joshua P. DiGangi

Thesis
for the
Degree of Bachelor of Science
in
Chemistry

College of Liberal Arts and Sciences
University of Illinois
Urbana-Champaign, Illinois

2006

Table of Contents:

<u>Acknowledgements:</u>

I would like to thank Prof. Ben McCall for all of his advice and for his confidence. I would like to thank Dr. Yun Ding for his assistance in setting up the wavemeter optics and with the design of the N_2^+ cell. I would like to thank Dr. Susanna L. Widicus Weaver and Brian Pohrte for their help with the spectrometer and general advice. I would like to thank Dr. Jim Wentz for his help with the electronics design. I would like to thank Easter Smith for making sure that I remember to have fun every once and a while. Most of all, I would like to thank my parents for both their financial and emotional support throughout my entire undergraduate career. This would not be possible without their help.

1) Inexpensive Interferometric Wavemeter for Visible/NIR Lasers

1.a: Introduction

With the use of tunable lasers, accurate techniques for wavelength calibration are essential. For the highest accuracy calibration, a reference cell containing a well-documented molecule is the standard method. However, without a rough calibration, the reference cell method of high accuracy calibration is usually extraordinarily difficult. One common solution to this problem is the use of a wavemeter to provide a rough wavelength calculation. Unfortunately, commercial wavemeters can be very costly. The wavemeter described in this chapter offers a low-cost alternative to a commercial wavemeter. It is a reasonably simple project, yet spanning a variety of areas convenient for a spectroscopist, such as optics, digital and analog electronics, and some simple machining. This makes it a project well-fitted for an undergraduate thesis or a beginning project for a first-year graduate student.

1.b: Theory

Our wavemeter is based on the concept of a Michelson interferometer (see figure 1-1). In a Michelson interferometer, a beamsplitter splits the monochromatic light source beam into two equal beams. The pathlength of one of the beams between the beamsplitter and its respective mirror remains constant, where as the pathlength of the other beam is varied at a constant velocity, v_m. As the beams reflect and recombine, they interfere with each other and shine onto a detector. The constructive interference vs. destructive interference is dependent on the beam with the varying mirror which brings the beam in and out of resonance with the other beam. If v_m stays constant, this produces a sinusoidal wave pattern of constructive interference peaks of light intensity and destructive interference valleys of light intensity. Figure 1-2 shows the resultant pattern, called a fringe pattern. Each peak is called a fringe.
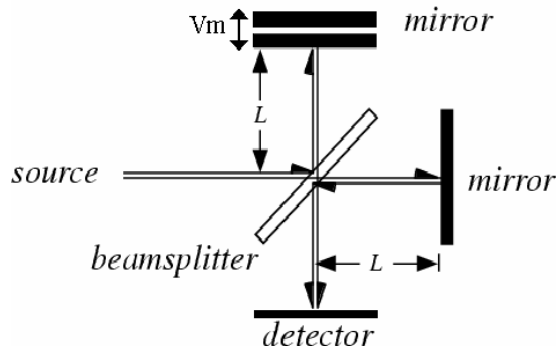
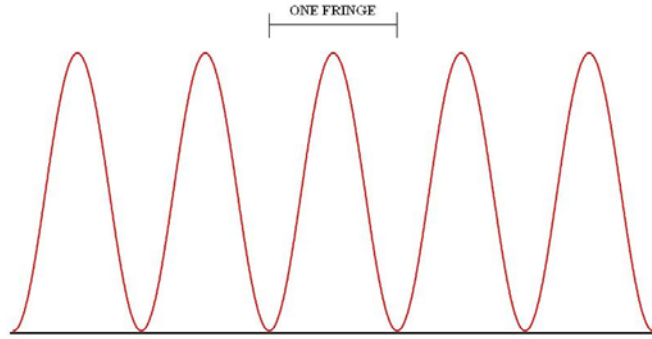**Figure 1-1 A Michelson Interferometer** [2]

Figure 1-2 A Fringe Pattern

The frequency of this fringe pattern is inversely proportional to the wavelength of light by the following relation.

$$f = 2 * v_m / \lambda \qquad (1\text{-}1)^{[3]}$$

However, the frequency of the fringe pattern divided by the velocity of the mirrors is simply equal to the number of fringes that appear, N, as the mirror moves a given distance, d_m.

$$f / v_m = N / d_m \qquad (1\text{-}2)$$

Combining equations 1-1 and 1-2 yields a relation between the number of fringes observed and wavelength.

$$d_m = 2 * N * \lambda \qquad (1\text{-}3)$$

Equation 1-3 allows for the determination of the wavelength of light by counting the number of fringes that appear while the mirror moves a certain distance. However, for this to be a practical means of laser wavelength determination, the accuracy the distance would need to be known is highly impractical.

Imagine instead, two lasers were placed running side-by-side, one laser with a well-known wavelength, λ_R, and the other laser with an unknown wavelength, λ_U. Since the distance the mirror moves is equal for both beams, the two equations can be set equal to each other, yielding λ_U as a function of the reference wavelength and the number of fringes from each laser.

$$\lambda_U = \lambda_R * N_R / N_U \qquad (1\text{-}4)$$

While this solves the distance accuracy problem, the distance itself remains a problem. For high accuracy measurements, many fringes need to be counted. For six significant figures, one million fringes must be counted. For a wavelength of one micron, this means the mirror must move a full meter. This is also impractical for most applications. However, if instead of one mirror moving, both mirrors move the same distance, then the distance they would have to move would be halved. The fringe frequency doubles for a given velocity of the mirrors. This system can be further simplified by having the mirrors attached, necessitating only one moving object. This is the reasoning behind the cart design detailed in 1.c.
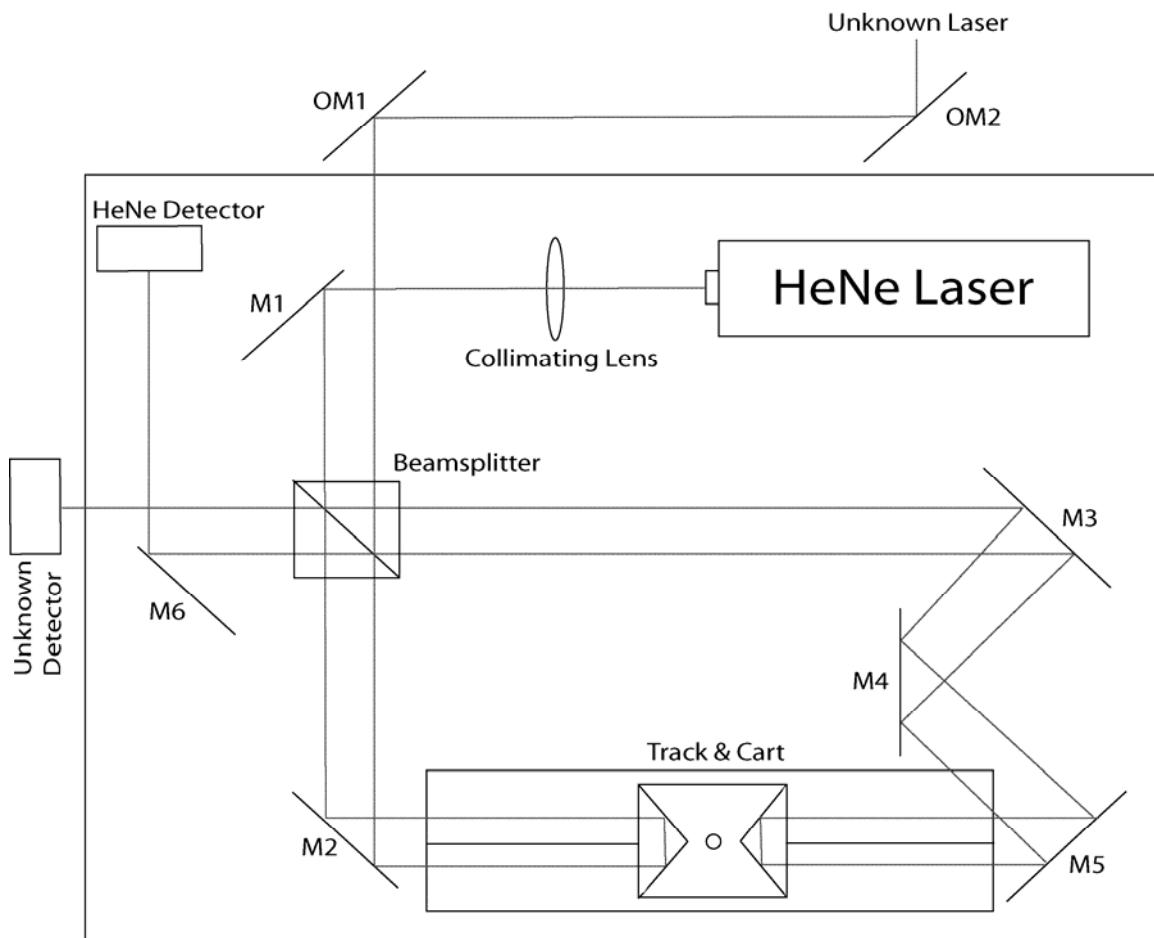
1.c: Mechanics/Optics

Figure 1-3: Wavemeter Schematic

Figure 1-3 shows a schematic of the wavemeter optics. The design is very similar to a two-beam Michelson interferometer. One major difference is that instead of one mirror moving there is a cart on a track that moves both arms at an identical rate. This cart, instead of having mirrors, is fitted with two cornercube prisms[*]. The effect of this is that when the return beams of the reference laser recombine at the beamsplitter[†], half of the recombined beam is sent on the path of the unknown laser. This makes alignment of the unknown laser beam as easy as making the two beams collinear. Another major difference is the use of three mirrors[‡] on the right arm. Two mirrors make the cart design possible; the third mirror simply adds another degree of freedom, easing alignment. All of the optics, with the exceptions of OM1, OM2, and the unknown laser detector, are mounted on a 2' X 2' X 3/8" aluminum plate. This allows for the wavemeter to be moved with only a minor realignment. The wavemeter uses 0.8 mW helium-neon (HeNe) laser[§] with a constant wavelength of 632823 pm as a reference laser.

The cart and track system used for this wavemeter was originally built from the design of P.J. Fox et.al.[1]. The cart and track were both built by the School of Chemical Sciences Machine Shop at the University of Illinois. Figures 1.4 and 1.5 show a schematic for the cart. This system calls for an air hose to be attached to the top of the cart. A channel ended by a metal tube extends from the top of the cylinder to channels in the legs of the cart. These channels lead to four 1 mm holes positioned on the inside bottoms of the legs. The cornercube prisms are mounted in the holes on each end of the cylinder and are each secured by a #8-32 Teflon screw. The cart is set on a highly polished aluminum track (see figure 1.6). Compressed air or nitrogen is forced out the four holes and suspend the cart on an air cushion. The reasoning behind using the cart as the source of floatation as opposed to using a track similar to an air hockey table is to

---

[*] EO Edmund – G43-297
[†] EO Edmund – G32-504
[‡] Mirrors M1 – M5 are from EO Edmund – G33-510. M6 is from Newark - 10D510. OM1 and OM2 are from ThorLabs – PF10-03-P01.
[§] EO Edmund – G61-337

maximize the consistency of the air pressure surrounding the cart. Pressure fluctuations change

the index of refraction of the air, causing changes in wavelength.
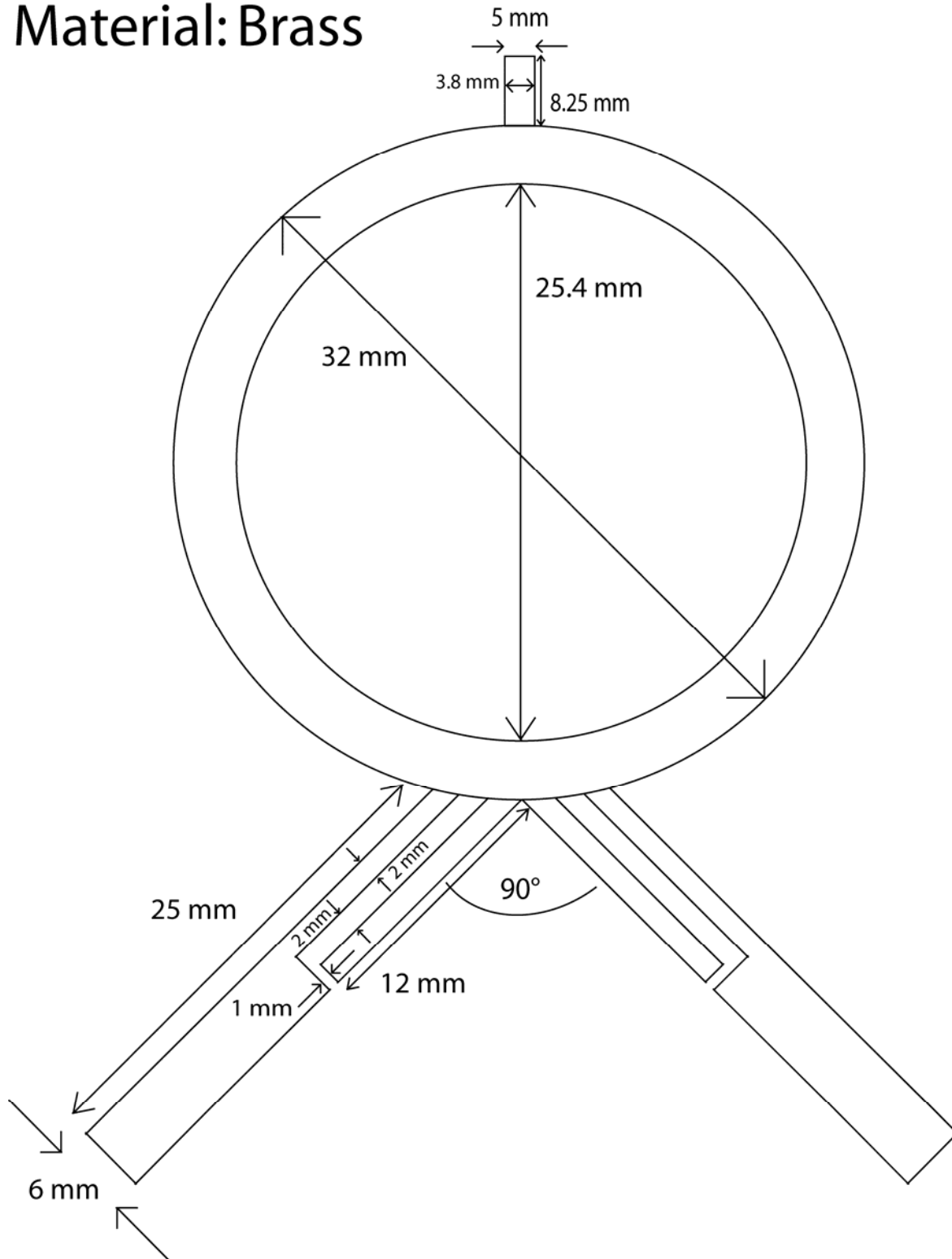

Material: Brass

5 mm

3.8 mm

8.25 mm

25.4 mm

32 mm

25 mm

2 mm

2 mm

90°

12 mm

1 mm
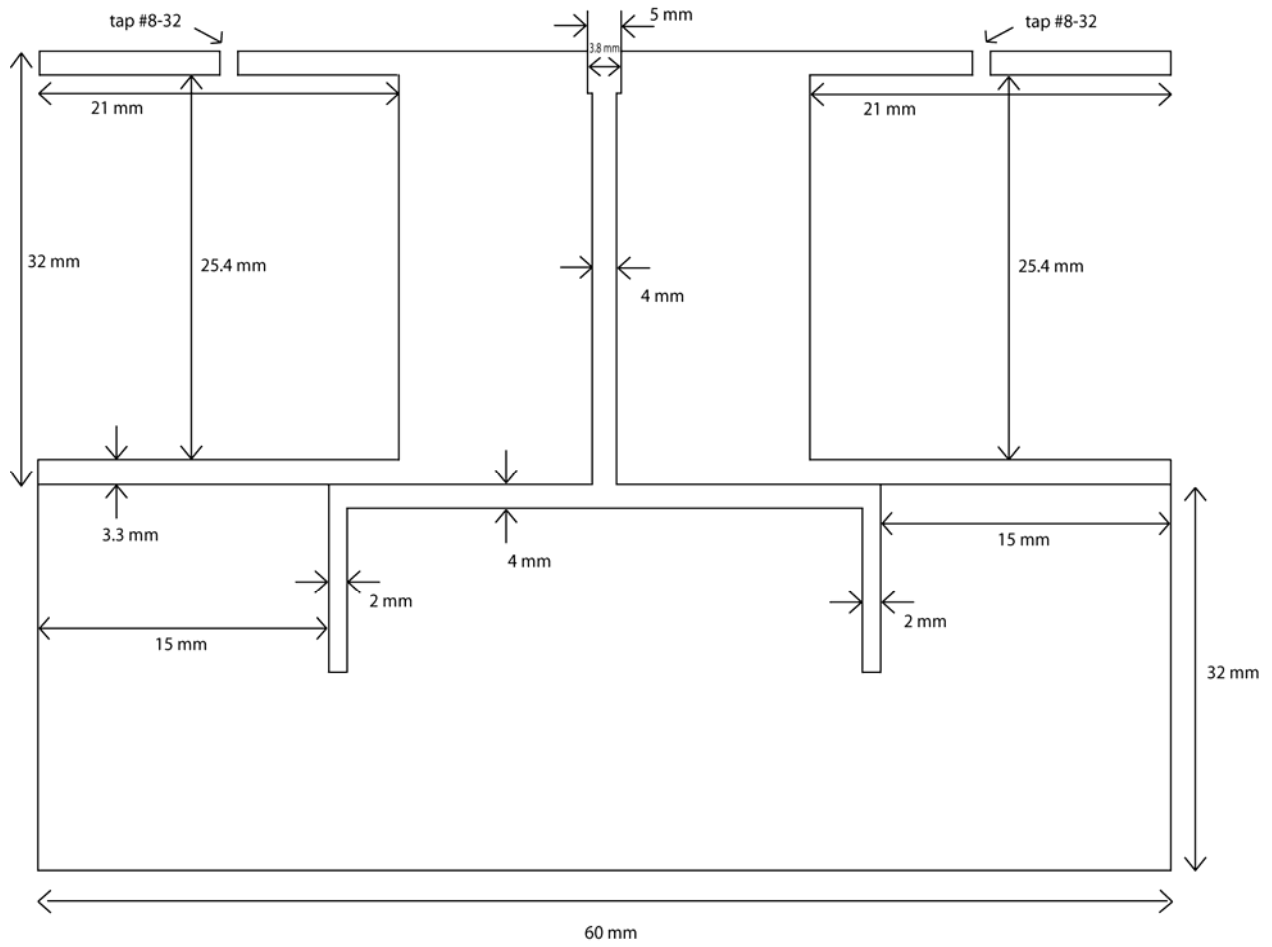
6 mm

Figure 1.4: Wavemeter Cart – End View

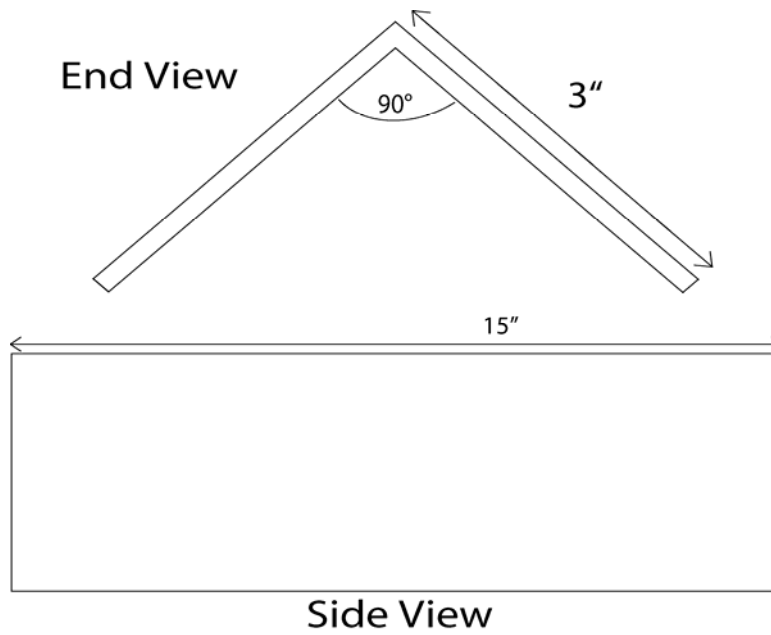**Figure 1.5: Wavemeter Cart – Side View**

Figure 1.6: Wavemeter Track

This system was found to work well to provide a frictionless surface. However, the cart also had a tendency to drift and/or move too quickly. The system was temporarily abandoned in favor of simply pushing the cart by hand. In this case, a piece of printer paper was taped to the track to reduce friction. The air system will be restored for the cart propulsion improvement discussed in section 1.g.ii.

The track is mounted to the plate using four anchors placed near each outside corner. The anchors were also built by the School of Chemical Sciences Machine Shop at the University of Illinois. Figure 1.7 shows a diagram of an anchor. Each anchor piece has four holes: one is tapped ¼"-20, one passes ¼"-20, and two are tapped #6-32. The hole that passes ¼"-20 is to mount the anchor to the board. The hole that is tapped ¼"-20 uses the force of a screw to prevent side to side motion of the track and hold the track to the board with pressure. The #6-32 holes are used for miscellaneous mounting needs, such as the reflective sensor arms.
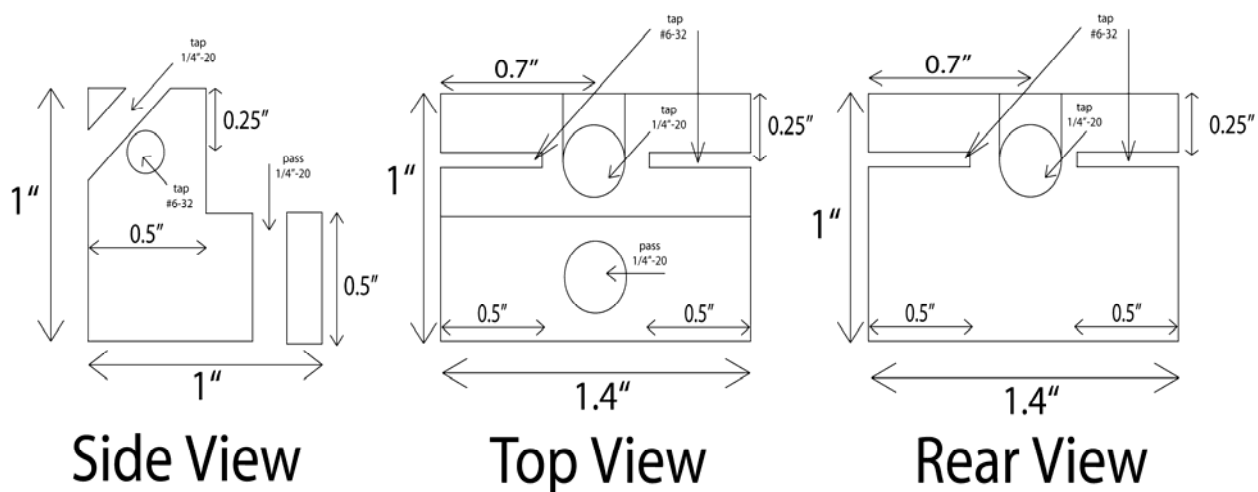
Figure 1.7: Track Anchors

The reflective sensors[*] are the means by which the counting circuitry is reset. When activated by the proximity of a reflective object, they send out a 5V signal. This allows them to interface with digital electronics, as shown in section 1.d. Originally, there was only one sensor. However, as will be explained in section 1.g.i., there are now two sensors, one on each side of

---

[*] Newark InOne – 52F4440

the track. The sensors are hung over the cart from arms attached to the #6-32 holes on the track anchors (see figure 1.8). The long arm is tightened against the anchor with a #6-32 screw. Another #6-32 screw is threaded through the slit on the short arm and screwed into the treaded hole at the end of the long arm. The slit allows the short arm to move parallel to the track. The sensor is fastened to the end of the short arm and placed so that when the cart is at one end, the sensor is over the leg of the cart, making the sensor activate. The sensor must be close enough to be triggered by the cart, but far enough so that it is not triggered by the track itself. To facilitate reflection, something somewhat reflective must be attached to the cart legs. The cart for this wavemeter uses a strip of white printer paper taped on the outside of each leg.

Material: 1/4" aluminum rod

2.7"

Tap #6-32

Pass #6-32

1.5"

Figure 1.8: Sensor Arm Schematic
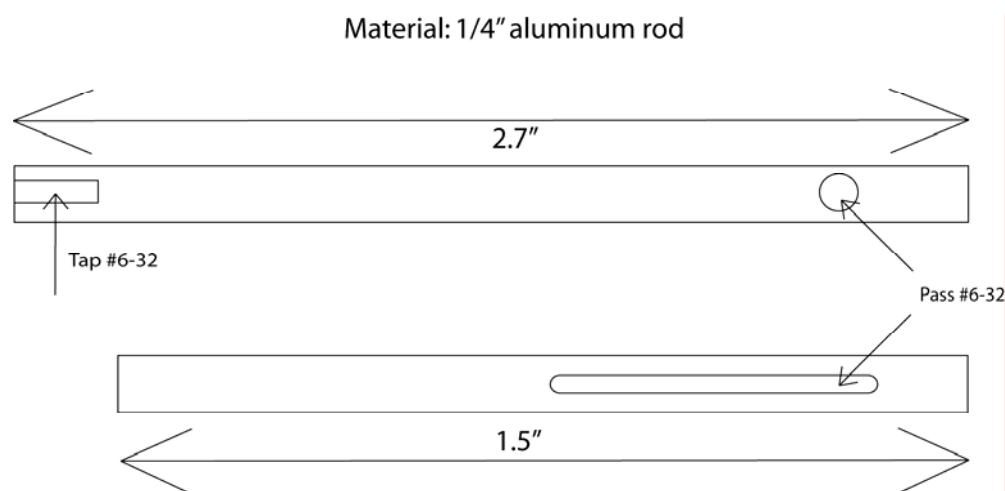
The wavemeter uses two different detectors. The detector for the reference laser is a DET110 from ThorLabs with an iris[*] attached. The DET110 is sensitive enough with a beam that provides a lot of AC signal, as the HeNe beam does. However, if the signal is not very large, there is a bandwidth problem. As the frequency of the fringe pattern, or the bandwidth, increases, the amplitude decreases. This provides an upper limit for cart speed for some detectors. Because of this, the DET110 is insufficient for many low power beams. The detector used in this wavemeter for the unknown laser is a Hamamatsu C5460 Series APD Module. The

---

[*] ThorLabs – SM1D12

Hamamatsu APD is much faster and has an adjustable gain, making it more than adequate for this application. The Hamamatsu APD also has the advantage for this wavemeter system of having a peak wavelength region nearer to that of the unknown laser than the DET110 (see section 2.d for more details about the unknown laser).

The HeNe laser is mounted on an aluminum plate supported by four 1" optics pillars[*]. The aluminum plate is made of ¼" aluminum stock and is about 10" X 3". There are four countersunk holes that pass ¼"-20. This allows a countersunk screw to fasten the pillars to the plate, which also screw into the base themselves. The platform is altogether is 1.25" tall, placing the plane of the beam almost dead center on the cornercubes. In addition to the countersunk holes, there are two holes that are tapped ¼"-20. These holes are used for brackets to hold the laser to the platform. This platform keeps the laser from moving with respect to the base.

Altogether, the optics make the following beam path. The HeNe beam first is collimated through a lens[†] placed about 5" from the front of the laser. The beam then reflects off of M1 toward the beamsplitter, which splits the beam in two. The transmitted beam continues to reflect off of M2 into the cornercube and is redirected back about a half of a centimeter to one side. It reflects off M2 again and rejoins the other beam at the beamsplitter. The reflected beam reflects off of M3, M4, and then M5 before coming to the other cornercube. The beam is also redirected about half a centimeter to the side and also reflects through M5, M4, and then M3 to rejoin the other beam at the beamsplitter. Once again, the beam splits in two. One beam reflects off of M6 into the reference detector. The other beam reflects off the beamsplitter and passes just to the right of M1. This is the beam used to align the unknown laser. The unknown laser travels the opposite path of the reference laser, causing one of the beams to pass to the right of M6 and enter the unknown detector.

---

[*] ThorLabs – PH1E
[†] EO Edmund – G45-280

1.d: Electronics

The wavemeter has four electronics boxes; two TTL converters, a main counting box, and a motor control box. The purposes of these boxes are to analyze the output fringe patterns of the two detectors and compare them to determine the wavelength. The motor control box is a part of the cart propulsion improvement and will be discussed in section 1.f.i.

The TTL converters (figure 1.10) were designed and built by Dr. Jim Wentz from the School of Chemical Sciences Computer Electronics and Electrical Services facility at the University of Illinois.   The goal of the TTL converters are to amplify the sinusoidal fringe pattern and then convert the fringe pattern to a pattern of square waves called TTL pulses.

Figure 1.9: Function of TTL converters

These TTL pulses are at 0 V, or ground, when low and at 5 V when high. They are used to represent binary numbers in digital electronics. A low signal is interpreted as a 0 and a high signal is interpreted as a 1. By converting the fringe pattern into a series of TTL pulses, digital electronics may be used to count fringes and perform the arithmetic to yield a wavelength.
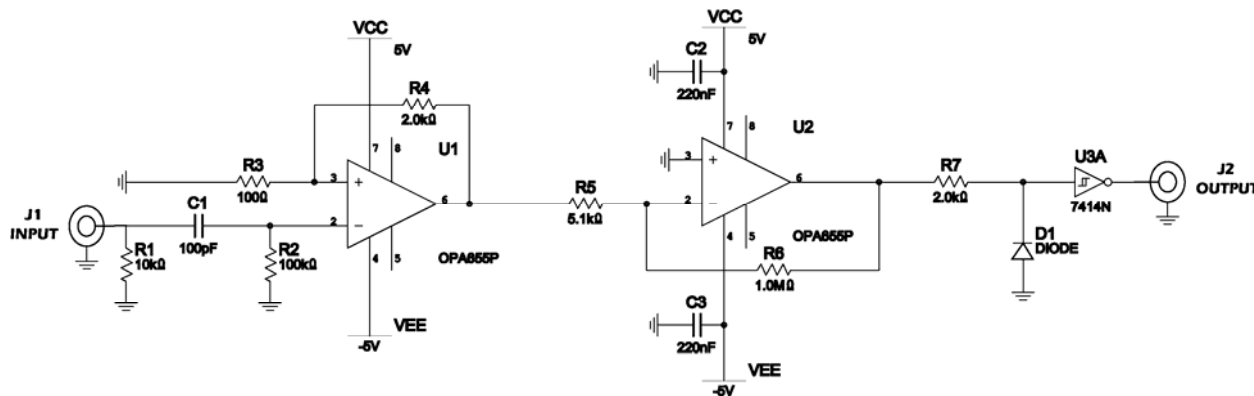

Figure 1.10: TTL converter schematic

The TTL converter uses two op-amps: the first amplifies the signal further and the second acts as a comparator to create TTL pulses. At the beginning, a capacitor removes any coupled DC voltage, leaving only the sinusoidal fringe pattern. At the end is a Schmitt trigger to yield a clean square wave. At each end is a BNC adaptor for connection to the detector or main electronics box. The BNC cable between the detector and its TTL converter should be either as short as possible or well shielded to decrease extra noise added to the system. During periods when the cart is not moving, the TTL converters should still output TTL pulses. This is from noise triggering the TTL converter, works by looking by detecting a 0 V crossing. For this reason, if the cart stops at any point while taking a reading, the reading is invalid.

The main electronics box is where the main circuitry for the wavemeter lies, including the counting circuitry. The counting circuitry is based on the counting circuitry from P.J. Fox et al.[1]. The unknown laser signal goes into 74LS193 chips, which are hexadecimal counters. Five 193's are used in series to count down from 9A7F7, which in base 10 is 632823, the wavelength of the reference laser in picometers. NAND gates in one of the 74LS00 chips are linked together to form a set-reset flip-flop. The unknown laser signal goes into this flip-flop, from which it goes into 74LS192 chips, which are decade counters. Six 192's are used in series to simply count up the number of reference laser pulses. When 632823 unknown laser pulses have been counted by the 193's, the MSD[*] 193-chip sends a pulse to the flip-flop, turning the reference signal off. The number of pulses recorded on the 192's then remains constant and is equal to the wavelength of the unknown laser. Six seven-segment LEDs are connected to the decade counters to display the current count at any given time.
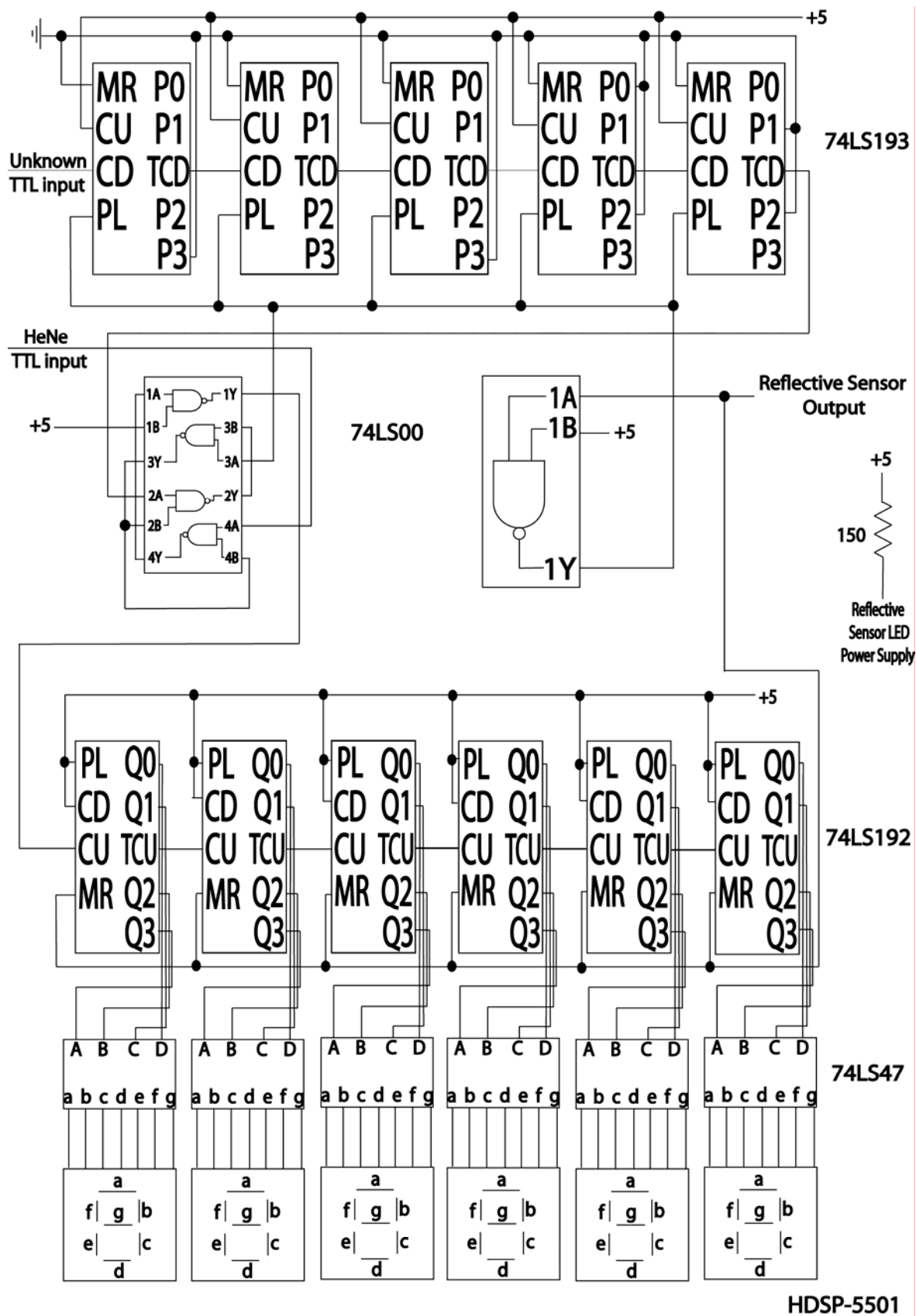
---

[*] MSD = Most Significant Digit

Figure 1-11: Wavemeter Main Box Electronics

Figure 1-11 shows the diagram for the electronics system in the wavemeter's main electronics box. The system is reset by a reflective surface sensor, as explained in section 1.c. The reflective sensor requires five leads: two are ground, one is Vcc, one is for the output signal, and one for the LED power supply. The output signal is connected to the resets for the 192's and the flip-flop and the preload for the 193's. The LED power supply needs a 150Ω resistor to limit current to the LED; otherwise, the LED would fail.
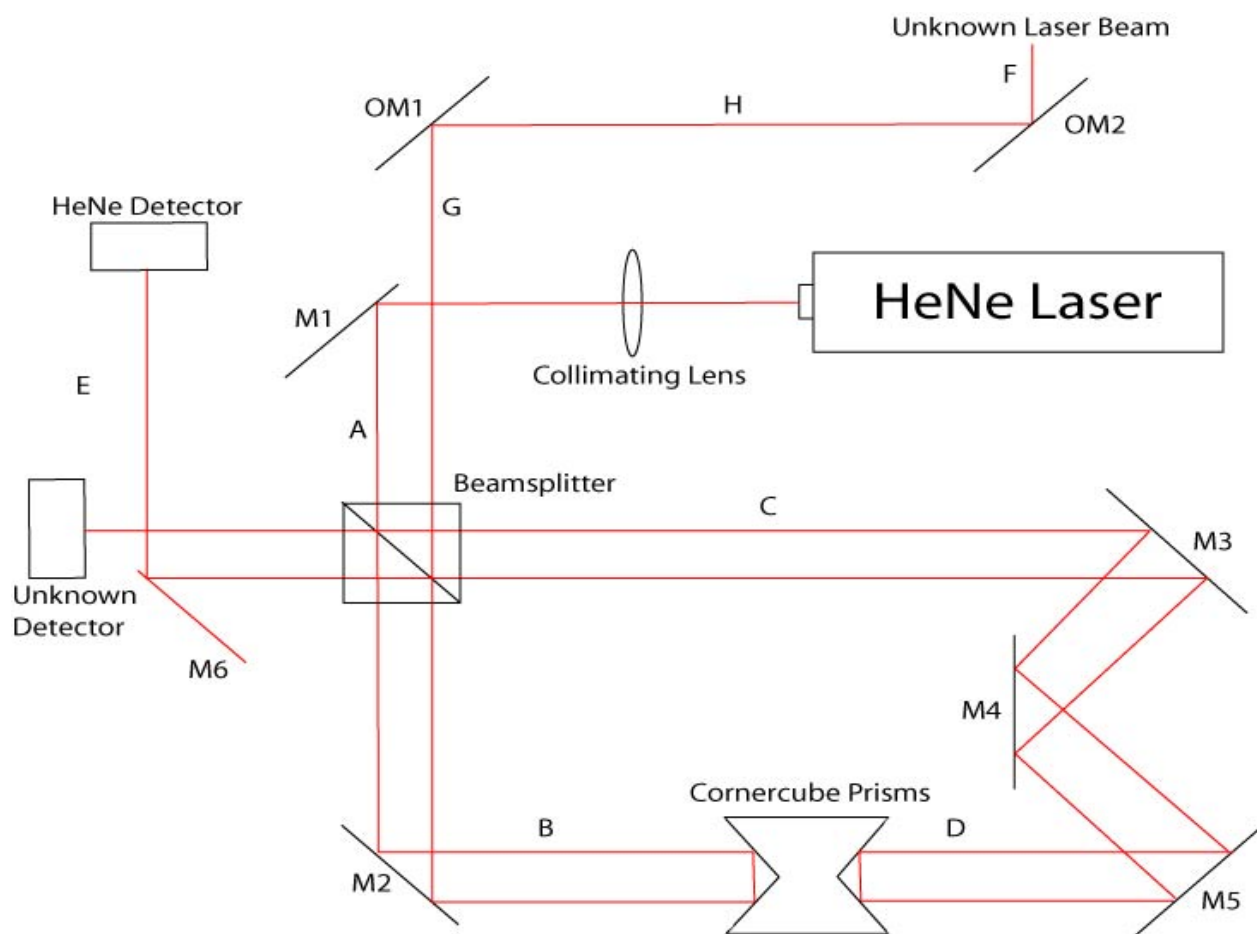
1.e: Alignment

Figure 1.z: Wavemeter Alignment Schematic

- Turn on all equipment (two detectors and the electronics box)
- Align inner mirrors
  - Block incoming "unknown" laser beam
  - Align beams A & B
    - Remove the cart with the cornercube prisms
    - Adjust M1 so that the HeNe beam runs perpendicular to the laser into the center of the beamsplitter
    - Adjust M2 so that beam B is directly above and parallel to the center of the track
    - Adjust M1 so that beam B is displaced from the middle toward the laser by about 0.5 - 1 cm
    - If not still parallel to the track, tweak M2
  - Align beams C & D
    - Obtain a thin piece of material, like a piece of lens cleaning paper
    - Check above the track for two beam spots: one caused by beam B and the other by beam D
    - Also check in beam C for two complementary spots
    - <u>Do not adjust M4 at this time!</u>
    - Adjust M5 to make the spots at beam C collinear and adjust M3 to make the spots at beam B/D collinear. Make only small adjustments at a time, for M3 and M5 still have a small effect on the other beam.
  - Align beam E
    - Replace the cart onto the track
    - Adjust M6 so that beam E centers on the iris
    - Place a card over the detector to more easily see the beam
    - If, when moving the cart, the beam(s) move:
      - Determine which beam is moving by blocking either B or C
      - Make small adjustments to M2, M3, and/or M5 to eliminate movement

- If you see two beams at the HeNe detector:
  - Make sure the beams aren't moving first (above)
  - Try to adjust M3 and M5 slightly so that the spots are collinear; if this just makes the spot move again, then return it as it was
  - Make a small adjustment to M4 so that the spots are <u>more</u> collinear
  - Realign beams C & D
  - Iterate the last two steps until the spots at B/D, C, and E are all collinear
- Remove the card and readjust M6 so that the beam is centered on the HeNe detector
- Close iris to a little less than the beam width and readjust M6
- Make sure beam E is hitting M6 as close to the edge as possible, as indicated in the diagram. If necessary, move and readjust M6

  o Either look at the signal out of the HeNe detector on an oscilloscope, or simply hook it up to the electronics and look at the readout. On the oscilloscope, on 2mV and 2.5 - 5 µs, you should see horizontal lines jumping up and down when the cart is not moving and a small sinusoidal pattern when the cart is moving continuously. On the electronics, simply look for smooth counting all the way across the track. If the numbers jump, stop, or slow down at any point and the cart was moving continuously, something is wrong. See troubleshooting for solutions.

- Align the outer mirrors
  o Unblock the "unknown" laser and block the HeNe beam at G
  o Adjust OM2 so that beam H hits roughly the middle of OM1
  o Unblock the HeNe beam
  o Adjust OM1 so that beam F hits near the center of the Faraday isolator in front of the "unknown" laser
  o Take the IR card and look for two spots each at F & G: one from the HeNe and the other from the "unknown"
  o Adjust OM1 so that the spots at F are collinear and adjust OM2 so that the spots at G are collinear. Do this using the same method as earlier: small adjustments

- Align the unknown detector
  - Attach the BNC output from the unknown detector to an oscilloscope
  - Look at the DC signal
  - Adjust the horizontal and vertical position of the detector separately to maximize the DC output (usually around 7 – 8 V)
  - The signal at ~2.5 μs time divisions should look like horizontal lines jumping up and down when you do not move the cart and strong, tall, sinusoidal peaks when you do.
- Reconnect the unknown detector output to the electronics and test the wavemeter. It should work!

1.f: Troubleshooting

--The numbers on the LEDs keep starting and stopping while moving the cart continuously.

Try going a little slower; a reading should take at least 3 seconds. If there is paper on the track, check to make sure that it is slick and not too greasy. If the cart does not slide really easy, change the paper. Try blocking the beam going into the unknown detector. If the numbers still skip, the problem is with the internal optics. Check the optics for dust or fingerprints, especially on the cornercubes. Then, realign the inner optics. Especially make sure the two spots on the reference detector are stationary while moving the cart and are superimposed. If after blocking the unknown laser beam the numbers stop skipping, then either the unknown detector and/or outer mirrors are out of alignment, or the unknown laser is unstable (i.e. mode hopping). Also, check that the iris is open about the size of the beam.

--The counters keep resetting when I try to move the cart.

Make sure the reflective sensors are an appropriate distance from the track and that they are tightly in place.

--The readout shows continuous numbers, but they are blatantly wrong.

Check the stability of the unknown laser. If it is stable, check the beam hitting the HeNe detector. If one of the beams moves as the cart goes from one side of the track to the other, adjust the appropriate mirrors (either M2 or M3 and M5) until it stops. If the beams do not move, but are also not collinear, adjust M4 as stated above. Check that the reference and unknown laser beams are collinear. Finally, check that the unknown detector is properly aligned.

1.g: Improvements

The goal for the wavemeter system has been to have a fully automated and accurate method of determining and recording laser wavelength. This goal is the reason behind some of the more recent improvements in the wavemeter system. One of the improvements is the automation of the cart, and has been referenced earlier a number of times. The other is a computer interface which sends the result of a wavemeter run, the unknown laser wavelength, directly to a computer.

1.g.i: Cart Automation

With the current system described in sections 1.b − 1.d, the wavemeter system still requires a person to manually operate it by pushing the cart across the track to take a reading. This is an unfortunate situation, for it would be preferable to remove the need for this person. To solve this problem, a system had to be devised to propel the cart across the track smoothly at a speed of about 3 seconds. It also must change direction automatically upon reaching the end.
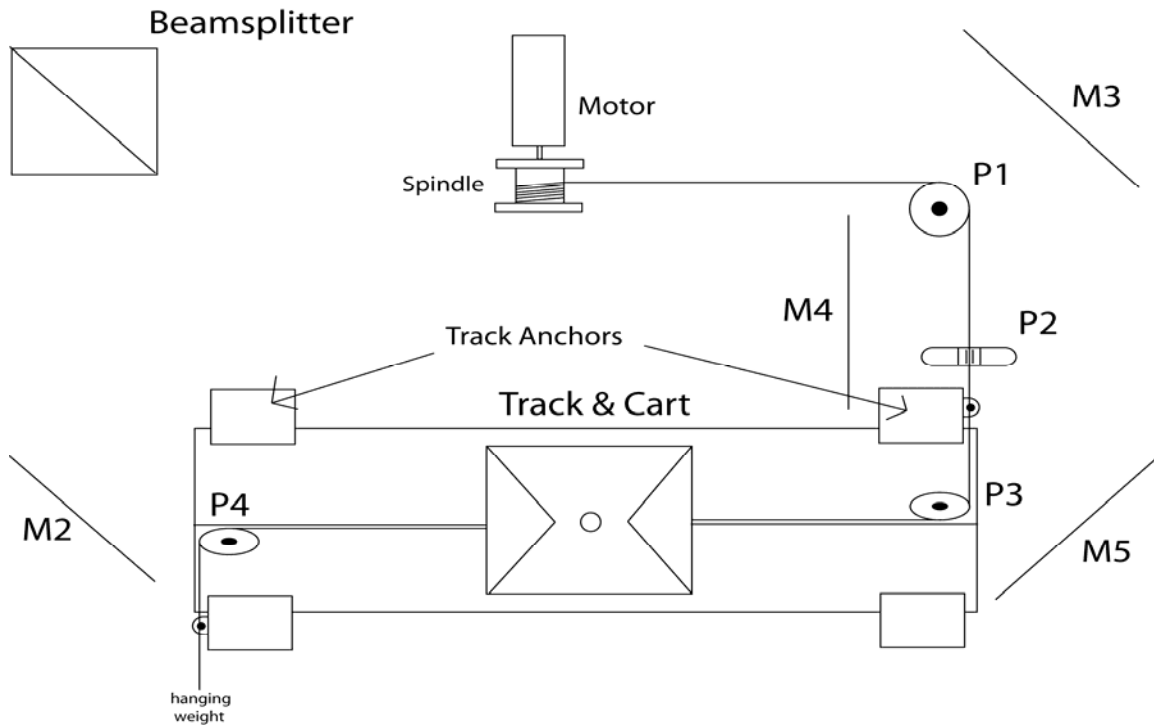
Figure 1.13: Cart Propulsion Schematic

Figure 1.13 shows the system devised for this purpose. A 5V DC gearbox motor[*] is attached to a spindle that winds a string, which is just kite string. The pulleys[†] were mounted to the track and board by tapping ¼"-20 holes into the track and board perpendicular to the surface and securing the pulleys using a very loosely-tightened ¼"-20 screw. P2 was simply mounted to the board also using ¼"-20 screws. Through these pulleys and an L-bracket[‡], the string runs from the motor to the cart, where the string is tied around the cart in the groove between the cylinder and the legs. Another string is tied to this "belt" around the cart, but on the opposite side from the other knot. This second string goes through another pulley and L-bracket, after which it is suspended from the table. This counterweight provides the force needed to pull the cart back while the motor unwinds. This allows for a string system, instead of a belt system which would be more difficult.

---

[*] 5V; 60:1 gear ratio; with gearbox, speed is ~60 RPM
[†] P1, P3, and P4 are the 25 mm pulleys in the Tamiya Pulley Set - #70141. P2 is from MSC - #67328385
[‡] The L-brackets are mounted underneath the sensor arms on both sides and are used as extra string guides. They are simply small L-brackets from an Erector set.
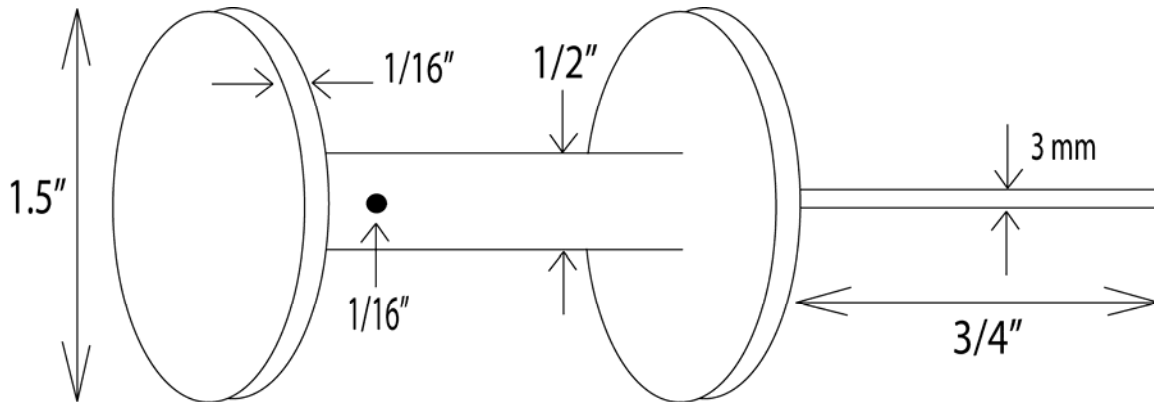
Figure 1.14: Spindle

The spindle was made by the School of Chemical Sciences Machine Shop at the University of Illinois. However, the material was brass and has proven to be a little soft. If the spindle were to be redesigned, stainless steel would be a much better material. An eyelet was milled in the middle through which to thread and tie the string. The spindle was attached to the motor using a male-male adapter sleeve which secures the both shafts with set screws.

Figure 1.15 shows a diagram of the electronics for the cart propulsion system. In order to change cart direction, the polarity of the voltage supply for the motor must be reversed. The polarity reversal for the motor is performed by a double-pull double-throw (DPDT) relay. The relay is switched by a set-reset flip-flop made from NAND gates. The flip-flop is set or reset by a high signal from one of the sensors. In addition, the sensor signals are connected to an OR gate, the output of which is wired to the reset signal in the main electronics box. Therefore, when either sensor is triggered, both the motor changes polarity, and in so direction, and the counters are reset. However, if the same sensor is triggered twice in a row, only the counters are reset and the motor maintains its same polarity, because the flip-flop remains in a constant state.
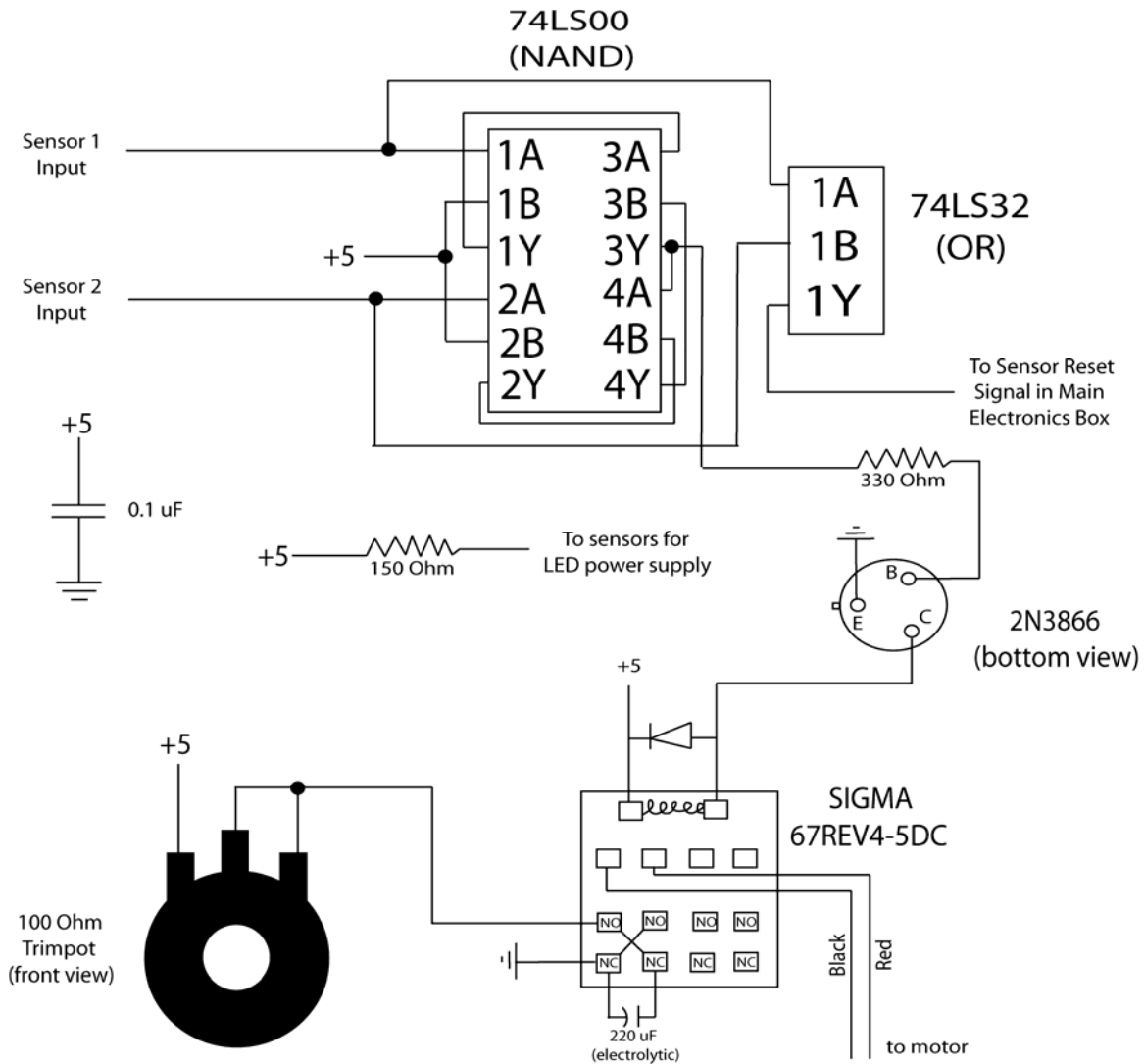
Figure 1.15: Cart Propulsion Electronics

In order for this system to work, the cart still needs to be frictionless. For this purpose, the air system has been resurrected. A piece of very elastic and flexible tubing is connected to the cart and suspended over the track to minimize force exerted on the cart by the tubing. The other end of this tubing is connected to a needle valve not far from the wavemeter. The needle valve is then connected directly to the house air with only an inline filter[*] to remove any grease, particulate, etc. This setup minimizes torque on the cart which is crucial to creating a frictionless air cushion.

---

[*] Grainger – #1A483

This system has been proven to work, but has not been implemented for long trials or in practice. Some problems have been detected already. For example, after running for a period of time, the motor will seem to get stuck. More testing will need to be done before this can be declared a properly functioning system.

1.g.ii: Computer Interface

Another improvement currently in the process of being implemented is a computer interface for the wavemeter. This will eventually involve not only reading in the unknown laser wavelength at a given time but also keeping a record of previous readings. This improvement would finally virtually eliminate the need for a person to watch the wavemeter.

To implement this, a 24 digital channel data acquisition (DAQ) card was obtained from National Instruments[*]. Buffering chips, 74LS214, have been placed on the main electronics board, through which the outputs from the decade counters are buffered to prevent feedback into the wavemeter electronics. The signals were then connected to a 50-pin ribbon cable which plugged into the connector. Table 1.1 provides a list of connections between decade counter outputs and DAQ ports.

Unfortunately, since the DAQ card has only 24 input channels, there is no room for a separate channel to indicate a reading has been taken. To fix this, a channel had to be freed by some means. Since the most significant digit always remains the same for the current application, the most significant bit, VI Q_A, was used as a trigger. In the control program, a constant value was set for this bit. The disadvantage to this is if another laser is used with the wavemeter, the value of the bit will have to be changed.

---

[*] PCI-6503

Decade Counter Output	DAQ Port
GND	GND
I Q_D	PC7
I Q_C	PC6
I Q_B	PC5
I Q_A	PC4
II Q_D	PC3
II Q_C	PC2
II Q_B	PC1
II Q_A	PC0
III Q_D	PB7
III Q_C	PB6
III Q_B	PB5
III Q_A	PB4
IV Q_D	PB3
IV Q_C	PB2
IV Q_B	PB1
IV Q_A	PB0
V Q_D	PA7
V Q_C	PA6
V Q_B	PA5
V Q_A	PA4
VI Q_D	PA3
VI Q_C	PA2
VI Q_B	PA1
VI Q_A	PA0

Least Significant Digit = I; Most Significant Digit = VI

Table 1.1: DAQ input connections

To finish this improvement, the DAQ card program and the unknown laser control program need to be connected. The difficulty behind this is that they are in two different computers. Efforts are currently underway to network these computers to send and store a history of readings.

2. Rovibronic Spectrum of the A-X 2-1 Band of N_2^+ using Cavity Ringdown Spectroscopy

2.a: Introduction

The A-X system of N_2^+ was first discovered by Meinel in 1950 while studying near-IR auroral emissions[4]. Ever since, this system, called the Meinel system, has been widely studied with various techniques. While important for atmospheric chemistry, N_2^+ is also important for its use as an inexpensive standard gas phase discharge molecule. With well documented, high resolution spectra, N_2^+ can be used to test new gas phase discharge sources and spectrometers. Unfortunately, there are yet many gaps in the spectrum; the 2-1 band is one of these gaps. This chapter describes an experimental setup with which to study this band. The experiment itself has not yet been completed. All information to date is included, as well as a description of future work
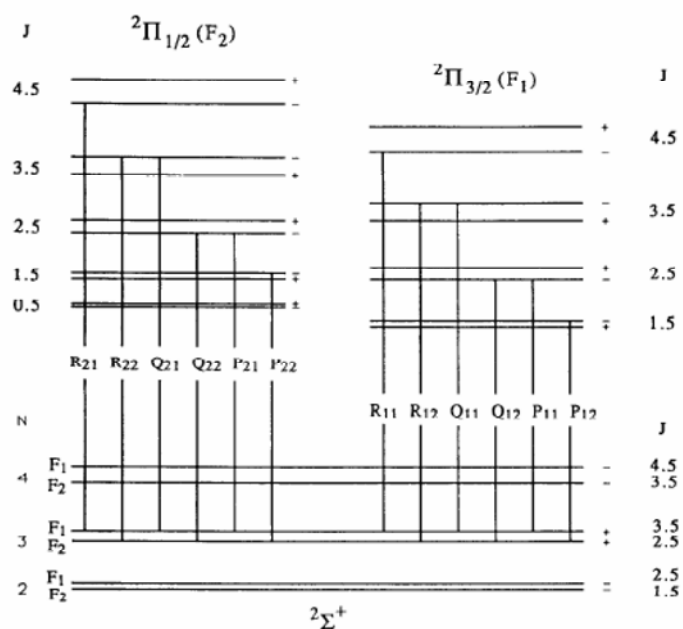
2.b: Theory

Figure 2.1: The Meinel System of N_2^+

Figure 2.1 displays the rotational level structure of the Meinel system. The excited state energy levels are split into two branches. This effect is caused by the spin-orbit coupling of the unpaired electron. If the projection quantum number of this electron's spin is 1/2, the projection of the total angular momentum of the molecule is 3/2, placing it in the right branch. If the projection quantum number of this electron's spin is -1/2, the projection of the total angular momentum of the molecule is only 1/2, placing it in the left branch. Each energy level also is exhibits a two-fold degeneracy which is caused by spin-rotation coupling. The spin-rotation coupling causes the electron spin to be either added or subtracted from the rotational quantum number, yielding half integral J-values.

In order to make a prediction of the spectrum, a method called combination differences was used with data obtained from Ferguson et.al.[4] and Bachir et.al.[5]. The method of combination differences uses experimental data to fill in gaps of unobserved lines. The ground state energies are calculated using experimentally determined rotational coefficients. The energies of the excited states are found by adding the transitions to the ground states. If there are enough observed lines, an energy should be obtained for most excited states. Finally, for all unobserved transitions, the ground state energy is subtracted from the excited state energy, yielding the frequency of the transition.

For example, assume that a molecule is being studied with the energy level structure as shown in Figure 2.2. Also, assume that the Q_2 transition is unobserved, while the R_1 transition is observed. Using the rotational constants for this molecule, the ground state energies for J=1 and J=2 can be found. By adding the ground state energy for J=1 to the energy of the R_1 transition and subtracting the ground state energy for J=2, the energy of the Q_1 transition can be easily found.
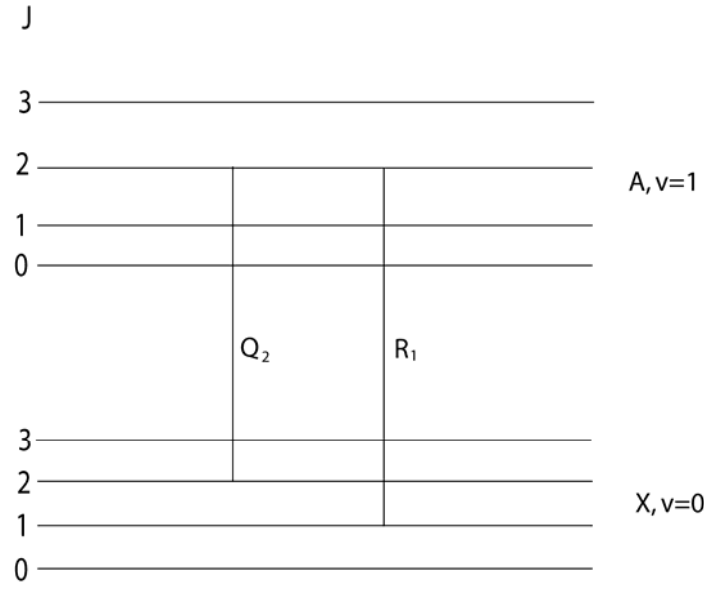
Figure 2.2: An Example of Combination Differences

For the A-X 2-1 band of N_2^+, the ground state energies (F_1 and F_2) were calculated for

v=0 and v=1 using constants and equations obtained from Ferguson et.al.[4].

$$F_1(N) = B_vN(N+1) - D_v(N(N+1))^2 + \tfrac{1}{2}\,\gamma_vN \tag{2-1}$$

$$F_2(N) = B_vN(N+1) - D_v(N(N+1))^2 - \tfrac{1}{2}\,\gamma_v(N+1) \tag{2-2}$$

The v=2 excited state energies were calculated by adding the transitions obtained from Bachir

et.al.[5] to the v=0 ground state energies. If any given excited state energy level had more than one

observed transition, the energies from each transition were averaged, and the average was used

as the energy for that level. The 2-1 transitions were then obtained by subtracting the v=2

excited state energies from the v=1 ground state energies.

Transition intensities were calculated using equations 2-3 – 2-15 from Earls[6].

$$i_{P22} = [(2J+1)^2 + U(2J+1)(4J^2+4J+1-2\lambda)] / (32(J+1)) \tag{2-3}$$

$$i_{P12} = [(2J+1)^2 - U(2J+1)(4J^2+4J+1-2\lambda)] / (32(J+1)) \tag{2-4}$$

$$i_{P21} = [(2J+1)^2 - U(2J+1)(4J^2+4J-7-2\lambda)] / (32(J+1)) \tag{2-5}$$

$$i_{P11} = [(2J+1)^2 + U(2J+1)(4J^2+4J-7-2\lambda)] / (32(J+1)) \tag{2-6}$$

$$i_{Q22} = [(2J+1)((4J^2+4J-1) + U(8J^3+12J^2-2J+1-2\lambda))] / (32J(J+1)) \tag{2-7}$$

$$i_{Q12} = [(2J+1)((4J^2+4J-1) - U(8J^3+12J^2-2J+1-2\lambda))] / (32J(J+1)) \qquad (2\text{-}8)$$

$$i_{Q21} = [(2J+1)((4J^2+4J-1) - U(8J^3+12J^2-2J-7-2\lambda))] / (32(J+1)) \qquad (2\text{-}9)$$

$$i_{Q11} = [(2J+1)((4J^2+4J-1) + U(8J^3+12J^2-2J-7-2\lambda))] / (32(J+1)) \qquad (2\text{-}10)$$

$$i_{R22} = [(2J+1)^2 + U(2J+1)(4J^2+4J-7-2\lambda)] / (32J) \qquad (2\text{-}11)$$

$$i_{R12} = [(2J+1)^2 - U(2J+1)(4J^2+4J-7-2\lambda)] / (32J) \qquad (2\text{-}12)$$

$$i_{R21} = [(2J+1)^2 - U(2J+1)(4J^2+4J+1-2\lambda)] / (32J) \qquad (2\text{-}13)$$

$$i_{R11} = [(2J+1)^2 + U(2J+1)(4J^2+4J+1-2\lambda)] / (32J) \qquad (2\text{-}14)$$

$$U = (\lambda^2 - 4\lambda + (2J + 1)^2)^{-1/2} \qquad (2\text{-}15)$$

where $\lambda = A/B = -74.63628 / 1.697384 = -43.97136^*$. Predicted intensities were then calculated using equations 2-16 and 2-17. g_D is the factor that compensates for nuclear spin coupling, the effect of which doubles the intensity of even N transitions.

$$I_{PQR} = i_{PQR} * g_D * (2N+1)\,(\Theta/T) * e^{-\Theta N(N+1)/T} \qquad (2\text{-}16)$$

where
$$\Theta = h * v / k_B \qquad (2\text{-}17)$$

This relatively simple model is able to give a rough estimate of line positions and intensities. As shown in figure 2.3, the model can be used to generate a stick spectrum of expected lines. One of the biggest downsides to this method is that it does not take into consideration the Gaussian shape of the peaks which will reduce the intensities. Also, this predicted spectrum is based on experimental data, meaning that experimental error is still present in and even may be compounded by this method. For example, sometimes two peaks cannot be resolved and results in a blended line. The peak of the blended line, and therefore the experimental frequency of the transition, is slightly off from both peaks. This can affect the average for the energy level, and thereby all of the transitions derived from that energy level.

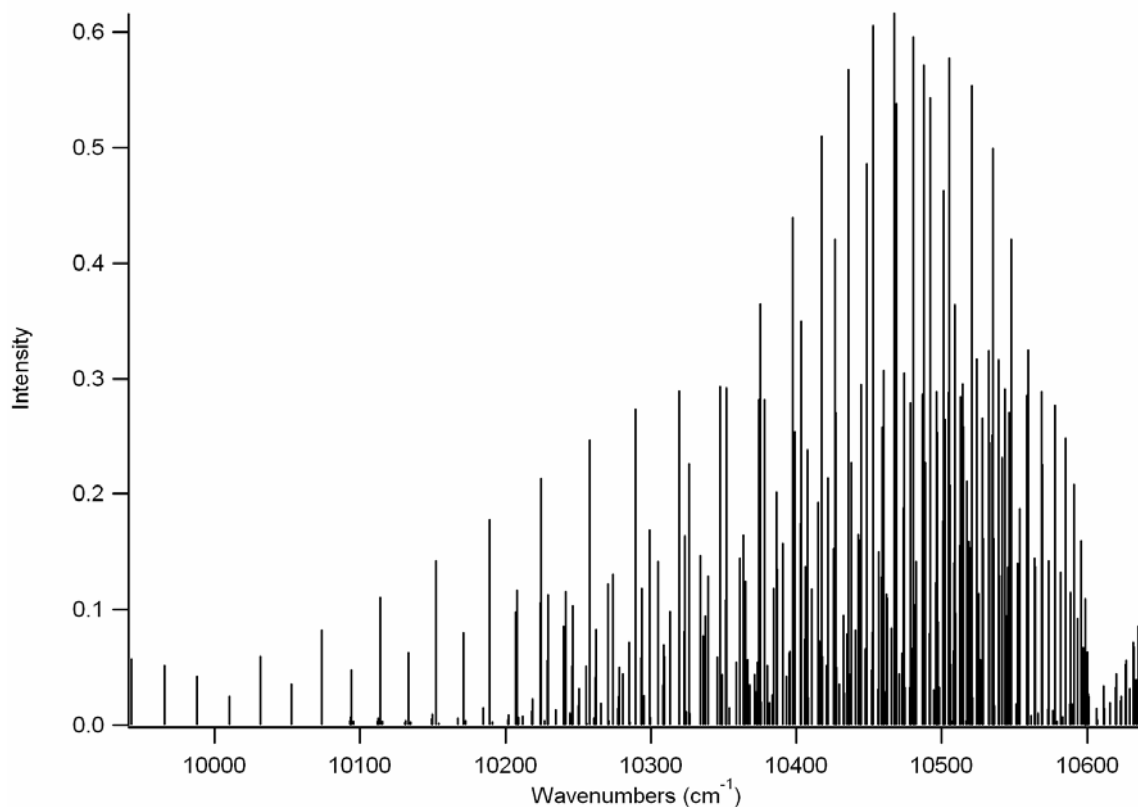* Values for A and B were the AΠ v=2 coefficients from Bachir et.al.[5]

Figure 2.3: Predicted Spectrum of A-X 2-1 band of N_2^+ at 800 K
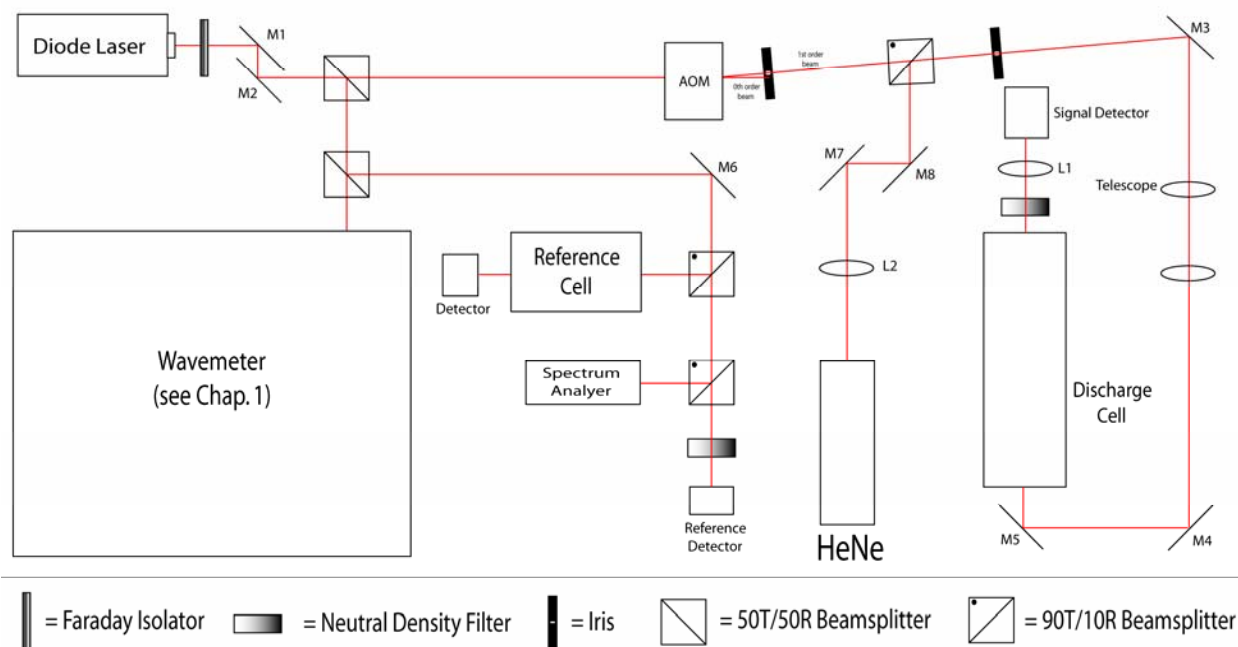
2.c: Experimental Setup

Figure 2.4: CRDS Spectrometer

Figure 2.4 shows the spectrometer which will be used to find the N_2^+ spectrum, which has been built by Dr. Susanna L. Widicus Weaver and Brian Pohrte. The spectrometer will use a tunable diode laser[*], which lases in the 0.92 – 0.98 µm region. Rough frequency calibration will be performed using the wavemeter described in Chapter 1, while the absolute wavelength calibration will be performed using a Herriot cell containing water as a reference molecule.

The technique that will be used is called Cavity Ringdown Spectroscopy (CRDS). CRDS is a high sensitivity direct absorption spectroscopic technique. CRDS uses two high reflectivity concave mirrors[†], one of which is controlled by a piezo-electric device. The mirrors are placed on opposing sides of the sample cell. The piezo voltage is swept up and down causing the distance between the mirrors, and therefore the cavity length, to change. The small leak of radiation from the mirrors is monitored using an APD detector[‡]. When the distance between the two mirrors hits an integral number of wavelengths, the cavity is at resonance, and the detector signal jumps. At this point, the piezo voltage is frozen, and the laser is deflected. The radiation experiences an exponential decay with time constant τ, which is recorded by the detector.

$$\tau = d / c[(1 - R) + \kappa(v)l] \tag{2-18}$$

Equation 2.18[7] displays how the time constant is dependent on the absorption coefficient, κ, and the frequency, v.

---

[*] Sacher Lasertechnik LiON Tunable Littman/Metcalf External Cavity Diode Laser
[†] Los Gatos Research - 901-0010-0950
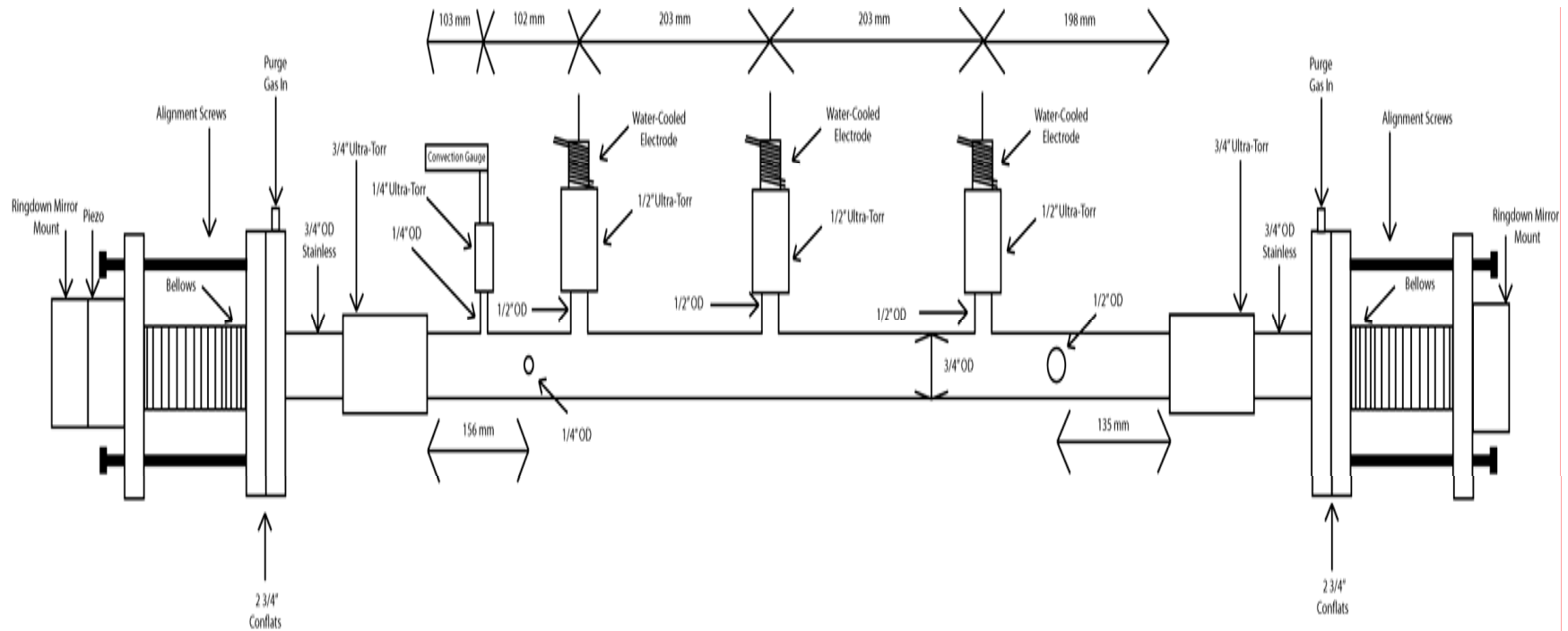[‡] Hamamatsu C5460 Series

Figure 2.5: N$_2^+$ Discharge Cell

Figure 2.5 shows a diagram of the discharge cell. It was made from Pyrex glass by the School of Chemical Sciences Glass Shop at the University of Illinois. The cell is ¾" in diameter with six flanges: four on the top and two in the front. The first flange from the left on the top is connected using an Ultra-Torr fitting to a convection gauge which is used to measure pressure. The other three flanges on the top of the cell are connected to electrodes. The electrodes are ½" Ultra-Torr fittings connected to a small piece of ½" steel rod wrapped with copper tubing. Water is run through the copper tubing to cool the electrodes. On the top of the electrode is attached a small rod of stainless steel where the power supply leads will be attached. In the front of the cell, the ¼" flange is connected by gas inlet, and the ½" flange is connected to the vacuum pumps. On each end, a ¾" Ultra-Torr fitting connects a ¾" stainless steel tube attached to a 2 ¾" conflat with a ¼" Swagelok intake for the purge gas on the top. The ringdown mirror mounts are attached to these conflats.

Two vacuum pumps are used are a Model 1402 and a Model 1405 Duo-Seal Welch vacuum pumps. From each pump, ½" Teflon tubing is run to a ½" Swagelok tee-connector, which then has another piece of ½" Teflon tubing attached to a ½" Ultra-Torr fitting which attaches to the ½" flange on the front of the cell. The power supply used will be from Universal Voltronics, model BAL 6-300-M. It is rated at 6 kV and 300 mA. Negative polarity is used to strike a discharge, because positive polarity causes arcing to the mirror mounts, which are grounded. Two 10 kΩ resistors are in series with the hot lead to limit the current of the discharge. The hot lead will be attached to the middle electrode, and the ground lead will be attached to the right electrode. The left electrode will float with no lead. This setup has been tested and is the only one that produces no arcing to the mirror mounts and no interference with the pressure gauge.

2.d: Plasma Characterization

Before an attempt can be made to obtain the spectrum of N_2^+, a prediction must be made of the conditions for which the maximum column density can be produced. In order to make this prediction, it was assumed that the column density of N_2^+ is proportional to the current of the plasma. Therefore, by comparing the current at different gas pressures and a constant voltage, a model can be made to predict where the current peaks. CO_2 was used as the purge gas due to the high voltage it requires to strike a plasma. N_2 was used as the source gas.

CO_2 Pressure (mTorr)	N_2 Pressure (mTorr)	Current (mA)	CO_2 Pressure (mTorr)	N_2 Pressure (mTorr)	Current (mA)
0	50	73	200	50	62
0	100	71	200	100	60
0	200	66	200	200	59
0	300	64	200	300	58
0	400	63	200	400	56
0	500	62	200	500	55
0	600	61	200	600	54
0	700	60	200	700	54
0	800	59	200	800	53
0	900	58	200	900	52
0	1000	57	200	1000	51
100	50	64	500	50	56
100	100	63	500	100	55
100	200	61	500	200	53
100	300	60	500	300	51
100	400	58	500	400	50
100	500	57	500	500	49
100	600	57	500	600	48
100	700	56	500	700	47
100	800	55	500	800	46
100	900	54	500	900	44
100	1000	54	500	1000	43

Table 2.1: Plasma Characterization Data @ 2000 V

Figure 2.6 shows the results of the plasma characterization in the form of a contour plot. The data showed that as the pressure of either gas increases, the plasma current decreases. This suggests that in order to maximize the column density of N_2^+, as little gas as possible with this system should be used.
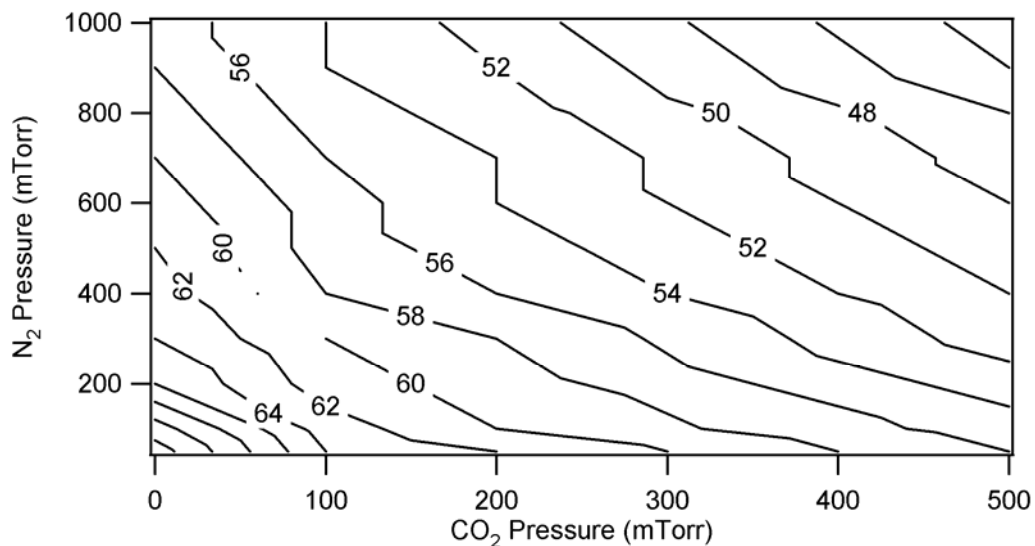
Figure 2.6: Contour Plot of Plasma Current (in mA) with respect to CO_2 and N_2 Pressures @ 2000 V

2.e: Future Work

Currently, two obstacles prevent the completion of this experiment. The first obstacle is the calculations necessary to focus the beam waist of the laser to the center of the cavity, or the mode matching calculations. The mode matching calculations will yield the foci and separation distance of the telescope lenses. With the help of Andrew Mills, these calculations are currently in progress but have yet to yield results.

The second obstacle is that the spectrometer is occupied for now with another experiment. Current plans dictate the spectrometer will be available for use for this experiment in June or July. Once the spectrometer is available, the frequencies corresponding to lines in the predicted spectrum will be scanned. Once N_2^+ lines are found, the gas pressures/ratios, initially set to comply with the plasma characterization prediction, will be adjusted for maximum column density. Lines will then be assigned by comparison with the predicted spectrum.

<u>References:</u>

1.   P.J. Fox, R.E. Scholten, M.R. Walkiewicz, and R.E. Drullinger, Am. J. Phys. **67**, 624-630 (1999).

2.   Motta, Leonardo. "Michelson Interferometer." <u>Eric Weisstein's World of Physics</u>. Ed. Eric Weisstein. **2006**. 17 April 2006. <http://scienceworld.wolfram.com/physics/ MichelsonInterferometer.html>

3.   Skoog, Douglas A., F. James Holler, and Timothy A. Nieman. <u>Principles of Instrumental Analysis</u>. 5th ed. Philadelphia: Harcourt Brace, **1998**. p185-187.

4.   D.W. Ferguson, K.N. Rao, P.A. Martin, and G. Guelachvili, J. Mol. Spec. **153**, 599-609 (1992).

5.   I. Bachir, H. Bolvin, C. Demuynck, J.L. Destombes, and A. Zellagui, J. Mol. Spec. **166**, 88-96 (1994).

6.   Lester T. Earls, Phys. Rev. **48**, 423-424 (1935).

7.   G. Berden, R. Peeters, and G. Meijer, Int. Rev. Phys. Chem. **19**, 565-607 (2000).

8.   David R. Lide, ed., *CRC Handbook of Chemistry and Physics, Internet Version 2006,* <http://www.hbcpnetbase.com>, Taylor and Francis, Boca Raton, FL, 2006.